Optimization of Topology of Multi Disc Aero Spike on Hypersonic Vehicles for the Reduction of Drag and Temperature at Blunt Nose Using CFD

[1]Kinthali Ravi Teja, [2]B. Keerthi, [3]Dr. M. Murali Krishna
[1]M.Tech scholar, [2]Assistant Professor, [3]Professor
[1,2,3]Department Of Mechanical Engineering,
Visakha Technical Campus, Visakhapatnam-530027, India

Abstract: Reduction of drag and heat load are two important aspects considered for hypersonic vehicles. To reduce the heat load, thermal protection system (TPS) is used. But the cost estimation of thermal protection system used in the hypersonic vehicles to reduce aero heating is very high. To overcome drag and heat load in hypersonic vehicles at low cost there is a need to find an alternative solution. So, by introducing a multidisc aerospike at frontal region of the hemispherical blunt nose of space vehicle, the drag and temperature can be reduced. By varying shape and geometry of multidisc of the aerospikes, its impact on performance is evaluated using best aerospike length to nose diameter ratio. Further, the combination of different geometries for the forward and intermediate disc yielded better results. Thus the thermal and drag reduction of a hypersonic vehicle is optimized and analyzed using fluent analysis under the characteristics of mach number, far-field pressure, velocity and temperature. Hence, from the results it was concluded that the combination of geometrical blunt nose with a triangular disc aerospike pointed edge facing away from the nose with an intermediate flat disc provides comparatively more amount of drag and temperature reduction of hypersonic vehicle.

Keywords: Thermal Protection System (TPS), Aerospike, Drag, Mach number, Blunt nose, fluent analysis

I. Introduction

To overcome drag and heat load in hypersonic vehicles at low cost there is a need to find an alternative solution. So, by introducing a multidisc aerospike at frontal region of the hemispherical blunt nose of space vehicle, the drag and temperature can be reduced. At first Alexanderin [1] suggested the use of aerospike for the Langley pilotless aircraft for the reduction of the drag on blunt body at supersonic speed. Bogdonoff and Vason [2] experimentally investigated that a flat face and a hemispherical cylinder aerospikes with *l*/*D* ratios in between 0 and 8 with a Mach 14. It was found that heat transfer to a spiked blunt body was reduced significantly. Crawford [3] investigated the effect of the aerospikes on aerodynamic heating and found that the rate of heat transfer was reduced when compared to un-spiked body when Reynolds number is low enough for existence of the laminar flow at reattachment point. Sudhir joshi et al.[5] concluded that flat triangular and flat disc aerospike with various l/D ratios at 6.2 Mach has reduced aerodynamic drag and heating. Gerdroodbary and Hosseinalipouralso[8] concluded that the aerospikes that are having the hemispherical tips are better for reducing the heat flux and aerospikes with the hemispherical tips having *l*/*D* ratio of 1 is optimum choice for both heat reduction and drag reduction. Holden [10] investigated on the spiked blunt bodies with different Mach numbers of 10 and 15 with *l*/*D* ratio of spike varying in between 0 and 4. Then suggested that, heat transfer rate at reattachment point is proportional to the reattachment angle. Khlevnikovon[11] investigated a spherical model that is equipped with a conical and a pyramidal aero disc of *l*/*D* ratio which is varying between 0·283 and 1·78 and shown that value of the peak heat flux will varies inversely with the distance from spike base. R.C. Mehta [14] has investigated the effect of forward facing aerospikes on the pressure and heat flux distribution over blunt body in numerical method. Stadler and Neilsonin[15] has studied the effect of aerospikes on the aerothermodynamics of a blunt body on the basis of heat transfer. It is observed that the combination of different geometrical disc shapes on aerospike is not available in literature.

II. Numerical Methodology

2.1 TO CALCULATE THE VELOCITY OF THE BLUNT BODY

Standard values at 13000m above sea level are:

Temperature (T) =216.65K

Pressure (p) =16510pa

Speed of sound (a) =295.07m/s

Density (ρ) =0.2655kg/m³

Mach number (M) = (speed of body) / (speed of sound in the surrounding medium) =v/a

Finding the velocity of blunt body at MACH number 8

For M=8,

M=v/A,

8=v/295.07,

v=2360.56m/s;

Velocity of the blunt body at Mach number 8 is 2360.56m/s.

2.2 TO CALCULATE THE DRAG ON THE BLUNT BODY

Calculation of the drag force on the blunt body at the velocity 2360.56m/s can be done based on the equation 2.1.

$$F_d = C_d \frac{\rho V^2 A}{2} \quad \text{Eq. (2.1)}$$

Where,

F_d = Drag Force in the direction of flow velocity

ρ = Density of the fluid

V = Flow speed

C_d = Coefficient of drag

A = Reference area

III. Geometrical Modelling

The main geometry represents hemispherical blunt nose having the diameter (D) of 40mm. The spike geometry consists of long cylindrical rod having radius 20mm which contains single and double disc aerospikes. Here, the aero disc contains different geometrical shapes which include flat triangular disc, triangular disc, hemispherical disc and flat disc. Firstly, an aerospike having single forward disc with different geometrical shapes having 6mm diameter is simulated. Secondly, along with the forward disc, a similar intermediate disc having diameter 8mm at different distances of 0.2l, 0.4l, 0.6l and 0.8l has been simulated. Finally, a triangular aero disc of 6mm diameter at front with an intermediate flat disc having diameter of 8mm at 0.4l (fig. 1.) has been simulated.

The dimensions of the required geometry are as follows :-

Table1. Dimensions of the blunt body

Diameter of the base body	D=40mm
Length of the base body	L=70mm
Diameter of spike	d=4mm
Length of the spike	l=80mm
Radius of aero disc	r=6mm, 8mm

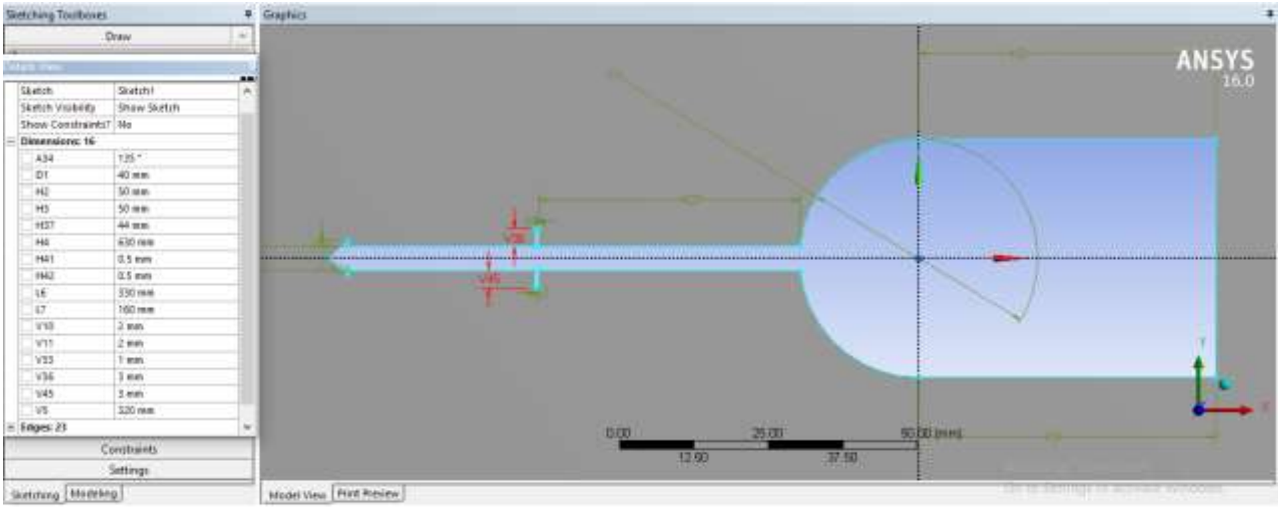

Fig. 1 Geometry of the body

IV. Mesh Generation

Meshing is the spatial division of the area into the cells called elements. Edge sizing controls can be given to any edge and allowed for different types of bias control, whereby the mesh size varies along the edge. The element size is given as 2.5e-004. The face sizing can be applied to any given face or a group of faces to control the mesh size on those particular faces. The element size in face sizing is given as 4.e-003m. The cell/element stacking can be achieved in a direction normal to the boundary using a feature called inflation. The maximum layers of 40 are given. Here, the specified parts are named as body and far-field. The geometry is selected and named according to the requirement. An unstructured mesh was generated with the addition of series of aero-spikes at the nose. The cell count for subsequent geometries varies from 3000 to 40000 quadrilateral cells depending on the length of the spike. Grids have been adapted to 110k to 140k cells based on the geometry during grid generation and flow gradient during simulation. The considered far-field conditions are given in table 2.

Table 2.Initial and far-field conditions

	Symbol	Units	Value
Mach number	M	-	8
Temperature	T	K	216.65
Pressure	P	N/mm^2	16066
Molecular viscosity	μ	Kg/m-s	$1.785x10^{-5}$
Reynolds number	Re	-	$1.01x10^{7}$

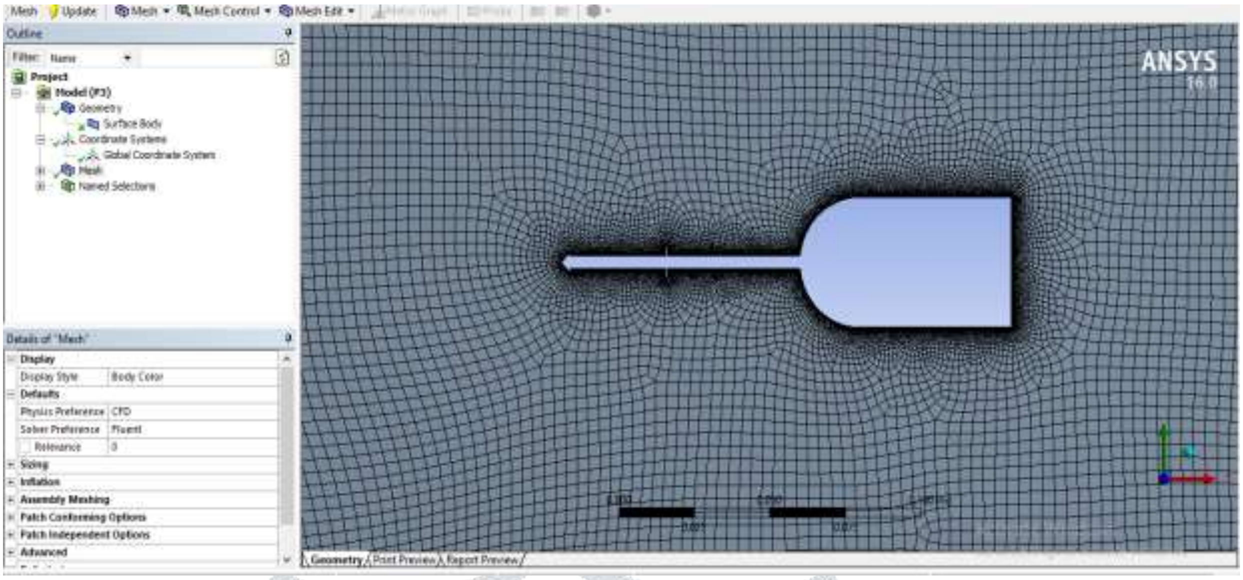

Fig. 2 Geometry of the body after meshing

V. Results and Discussion

Numerical simulations have been carried out for flat triangular disc, triangular disc, hemispherical disc and flat disc spiked blunt body. As shown in drag bar chart in figure3, a significant reduction in drag can be seen with the application of aero-spikes at the nose for all cases investigated. Temperature changes and drag changes due to the introduction of spike are given in teble3.

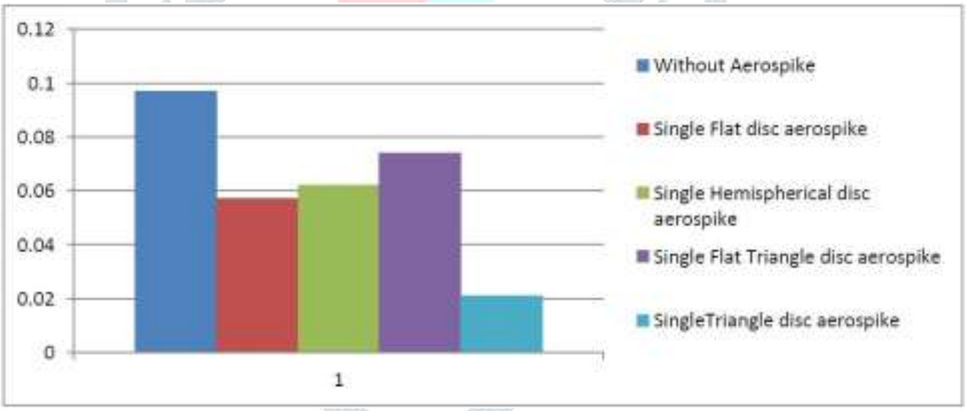

Fig. 3 Drag bar chart for single disc aerospike

Table 3. Changes of temperature and drag coefficient for single disc aerospike

Geometry	TEMPERATURE	Drag Coefficient
Blunt body without Aero Spike	1830˚k	Cd = 0.097
Blunt body with Flat Disc Aero Spike	1850˚k	Cd = 0.057
Blunt body with Triangle Disc Aero Spike	2870˚k	Cd= 0.021
Blunt body with Hemispherical Disc Aero Spike	2920˚k	Cd= 0.062
Blunt body with Flat Triangle Disc Aero Spike	2910˚k	Cd= 0.074

Among the flat triangular disc, triangular disc, hemispherical disc and flat disc spiked blunt body, flat disc and triangular disc aero spike are more effective in reducing the drag coefficient, which in turn reduces the drag. So, by taking those as reference models, double disc aerospike blunt nose has been designed with varying the space between the discs as 0.2l, 0.4l, 0.6l, 0.8l. So, again 8 models were developed and simulated for the drag coefficient reduction. From the drag bar chart for the flat double disc aerospike blunt nose in figure4, it is observed that arrangement of flat double disc aerospike with intermediate distance of 0.6l is reducing the drag coefficient effectively to 0.018. The temperature and drag coefficient values of the flat double disc aerospike blunt nose are shown in table4.

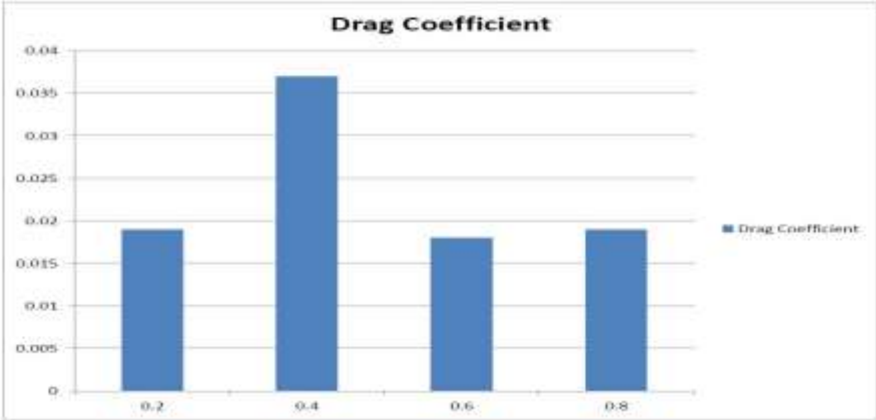

Fig. 4 Drag bar chart for flat double disc aerospike

Table 4. Changes of temperature and drag coefficient for flat double disc aerospike

GEOMETRY	TEMPERATURE	DRAG COEFFICIENT
Flat Double Disc at 0.2l	2910˚k	Cd= 0.019
Flat Double Disc at 0.4l	1860˚k	Cd = 0.037
Flat Double Disc at 0.6l	2970˚k	Cd = 0.018
Flat Double Disc at 0.8l	2980˚k	Cd = 0.019

Similarly from the drag bar chart for the triangular double disc aerospike blunt nose in figure5, it is observed that arrangement of triangular double disc aerospike with intermediate distance of 0.4l is reducing the drag coefficient effectively to 0.015. The temperature and drag coefficient values of the triangular double disc aerospike blunt nose are shown in table5.

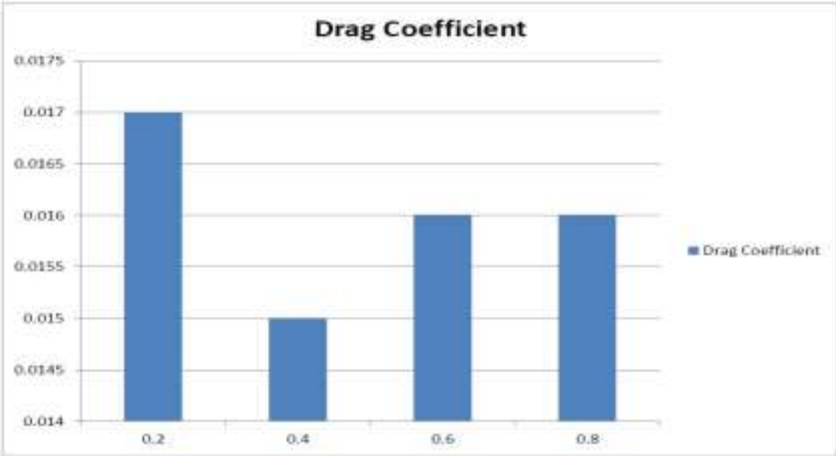

Fig. 5 Drag bar chart for triangular double disc aerospike

Table 5. Changes of temperature and drag coefficient for triangular double disc aerospike

GEOMETRY	TEMPERATURE	DRAG COEFFICIENT
Triangle Double Disc at 0.2l	2840˚k	Cd = 0.017
Triangle Double Disc at 0.4l	2790˚k	Cd = 0.015
Triangle Double Disc at 0.6l	2850˚k	Cd = 0.016
Triangle Double Disc at 0.8l	2900˚k	Cd = 0.016

Then the combination of triangular disc and flat disc has been prepared by placing the flat disc as an intermediate disc at a distance of 0.4l from the front disc. And this geometry is simulated for the coefficient of drag and temperature values. Results and distribution of temperature distribution, pressure distribution, velocity distribution and convergence of drag coefficient are shown in figures6, 7, 8, 9 respectively.

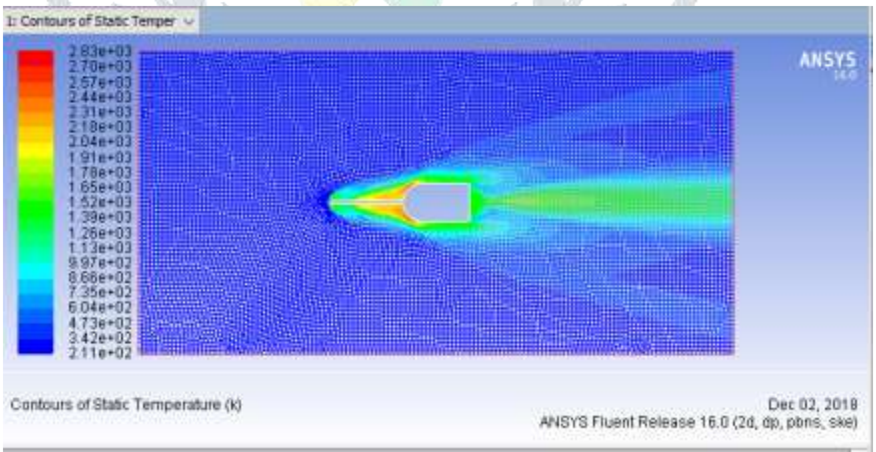

Fig. 6 Temperature distribution of Aerospike with triangular disc at front and flat intermediate disc at 0.4l

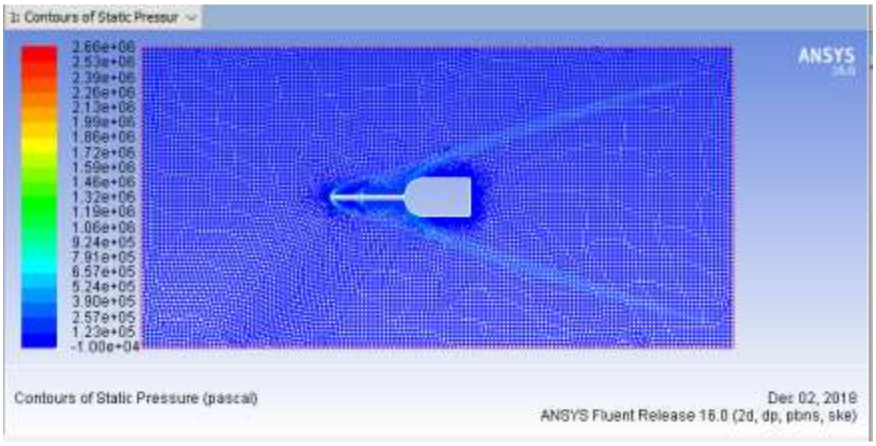

Fig. 7 Pressure distribution of Aerospike with triangular disc at front and flat intermediate disc at 0.4l

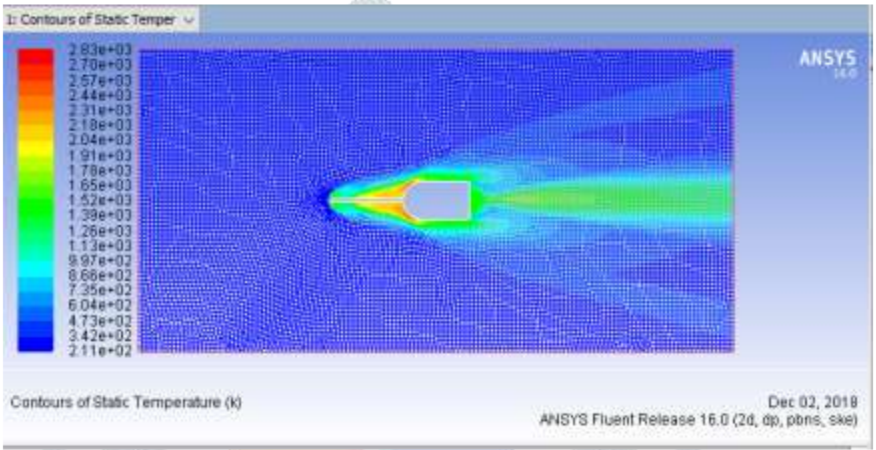

Fig. 7 Velocity distribution of Aerospike with triangular disc at front and flat intermediate disc at 0.4l

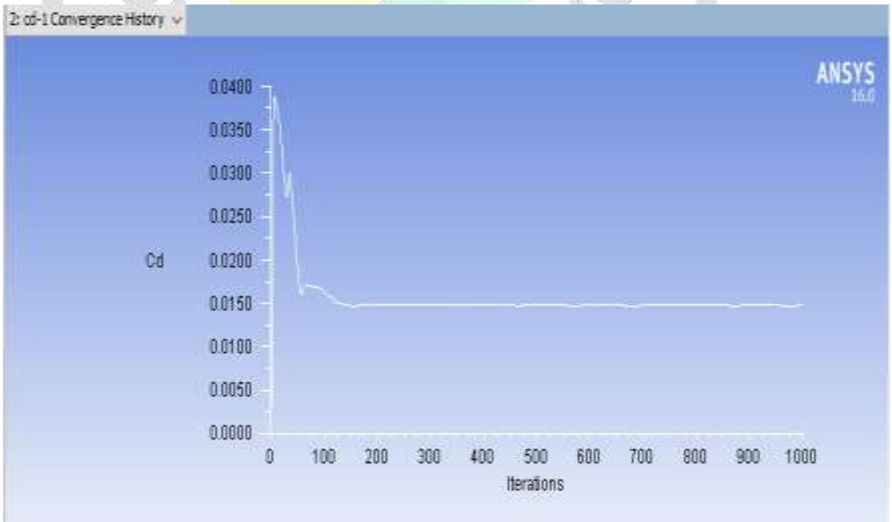

Fig. 8 convergence of drag coefficient for Aerospike with triangular disc at front and flat intermediate disc at 0.4l

Table 6. Maximum temperature and drag coefficient for triangular disc at front and flat intermediate disc at 0.4l

GEOMETRY	TEMPERATURE	DRAG COEFFICIENT
Triangular End with intermediate Flat disc Aero Spike at 0.4L	2830°k on disc 1700°k on blunt body	Cd = 0.014

Table 7. Maximum Velocity and Maximum Pressure for triangular disc at front and flat intermediate disc at 0.4l

GEOMETRY	Maximum Velocity	Maximum Pressure
Triangular End with intermediate Flat disc Aero Spike at 0.4L	2360 m/s	2.66 MPa

VI. Conclusion

It is clear from the results that the triangular disc with the pointed edge facing away from the nose gives more drag reduction when the intermediate flat disc is placed at an approximate position of 0.4l. The coefficient of drag at this position is 0.014. The temperature of the blunt body at this position is 2830°k on disc and 1700°k on nose of the blunt body. And the maximum achievable velocity is 2360 m/s which is almost equal to the theoretically calculated velocity of the hypersonic vehicle at Mach number 8. So, the reduction of drag force over the blunt body and drop in heat load is achieved by optimizing the geometry of multi disc aerospikes on the hypersonic vehicle.

References

[1] Alexander, S.R. Results of tests to determine the effect of conical windshield on the drag of a bluff body at supersonic speeds, January 1947, NACA RM L6K08a.
[2] Bogdonoff, S.M. and VAS, I.E. Preliminary investigations of spiked bodies at hypersonic speeds, J Aerospace, 1959.
[3] Crawford, D.H. Investigation of the flow over a spiked nose hemisphere –cylinder, December 1959, aerospace sciences, 1959.
[4] Effect of blunted aero disk on aero spiked blunt cone nose at high speeds. International research journal of engineering and technology-volume: 02 issue: 09; December 2015.
[5] Effect of double disk aero spikes on aerothermodynamics of blunt body at mach 6.2. International journal of applied engineering research ISSN 0973-4562 volume11, number1 (2016).
[6] Heubner , L.D., Mitchell, A.M. and Boudreaux, E.J. experimental results on the feasibility of an aero spike for hypersonic missiles, January 1995.
[7] Gauer, M. and Paull, A. numerical investigation of a spiked blunt nose cone at hypersonic speeds, J Space crafts and rockets , 2008.
[8] Gerbroodbary, M.B. and Hosseinalipour, S.M. numerical simulation of hypersonic flow over highly blunted cones with spike, Acta Astraonautica , 2010
[9] Heubner, L.D., Mitchell, A.M. and Boudreaux, E.J. experimental results on the feasibility of an aero spike for hypersonic missiles, January 1995.
[10] Holden, M. experimental studies of separated flows at hypersonic speeds, part i-separated flows over axis symmetric spiked bodies, 1996.
[11] Khlebnikov, V.S. distribution of heat flux on the surface of a sphere with a forward separation zone, fluid dynamics, 1986.
[12] Motoyama, N., Mihra K., Miyajima, R., Watanuki, T. and Kubota, H. thermal protection and drag reduction with use of spike in hypersonic flow, 2001.53
[13] Pavlovic, Milicev, influence of spike shape at supersonic flow past blunt nose bodies: experimental studies, 2001.
[14] R.C. Mehta, R.C. and Rathakirshnan , E. drag reduction for spike attached to blunt nosed body at mach6, J Space craft and rockets , 2010.
[15] Stadler , J. R. and Neilson , H.V. and heat transfer from a hemisphere cylinder equipped with flow separation spikes , 1954.
[16] Properties of the International standard atmosphere (ISA) between sea level and 20km geo potential altitude table.
[17] Vehicles using aero spike; International journal of research in aeronautical and mechanical engineering .vol5; issue1; Jan 2017.
[18] Governing equations of fluid dynamics, J.D.Anderson , Jr.
[19] www.cfd-online.com.